JOC*Article*

Competing Excited State Intramolecular Proton Transfer Pathways from Phenol to Anthracene Moieties

Nikola Basarić† and Peter Wan*

Department of Chemistry, Box 3065, University of Victoria, British Columbia, Canada, V8W 3V6

pwan@uvic.ca

Received November 30, 2005

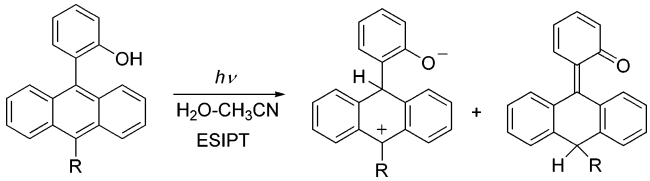

Four new 9-(2′-hydroxyphenyl)anthracene derivatives **7**−**10** were synthesized and their potential excited state intramolecular proton transfer (ESIPT) reaction investigated. Whereas **7** reacted via the anticipated (formal) ESIPT reaction (proton transfer to the 10-position of the anthracene), derivatives **8**−**10** reacted via ESIPT to both 9- and 10-positions, giving rise to two types of intermediates, quinone methides (e.g., **29**) and zwitterions (e.g., **30**). These intermediates are trapped by solvent (water or methanol) giving addition products that can readily revert back to starting material. However, on extended photolysis, the products that are isolated can best be rationalized as being due to competing elimination and intramolecular cyclization of zwitterions **30** and **37**. These results show that it is possible to structurally tune ESIPT in (hydroxyphenyl)anthracenes to either result in a completely reversible reaction or give isolable anthracene addition or rearrangement products.

Introduction

Excited state intramolecular proton transfer (ESIPT) is a fundamental process that has received considerable attention[1] since its first discovery by Weller.[2] ESIPT arises when a molecule contains both an acidic and a basic site which upon electronic excitation experience an enhancement in acidity or basicity, respectively. In most examples of ESIPT processes an OH or NH is the acidic site, while a basic site usually contains a heteroatom such as heterocyclic nitrogen or a carbonyl group. Since most of the ESIPT processes are reversible, these systems have found applications as photostabilizers,[3] laser dyes,[4] scintillators,[5] and solar collectors.[6]

We recently reported the first examples of ESIPT between phenol as an acidic site and an aromatic carbocyclic ring as a basic site.[7] These ESIPT reactions require initial hydrogen bonding interaction between the phenol OH and the π-system of the adjacent ring that is possible only in twisted biaryl structures.[7a] In the excited singlet state, the phenolic proton becomes sufficiently acidic to facilitate proton transfer to a carbon atom of an adjacent aromatic ring, giving rise to quinone methide (QM) intermediates (as shown in eq 1 for the parent system, 2-phenylphenol (**1**)[7a]). In the (hydroxyphenyl)anthracene (HPA) system **4**, water-mediated proton transfer to position 10 of the anthracene ring gives quinone methide **5**. The later is

* Address correspondence to this author.
† On leave from the Ruder Boškovic Institute, Zagreb, Croatia.

(1) (a) Ireland, J. F.; Wyatt, P. A. H. *Adv. Phys. Org. Chem.* **1976**, *12*, 131. (b) Klöpffer, W. *Adv. Photochem.* **1977**, *10*, 311. (c) Arnaut, L. G.; Formosinho, S. J. *J. Photochem. Photobiol., A* **1993**, *75*, 1. (d) Formosinho, S. J.; Arnaut, L. G. *J. Photochem. Photobiol., A* **1993**, *75*, 21. (e) Ormson, S. M.; Brown, R. G. *Prog. React. Kinet.* **1994**, *19*, 45. (f) Le Gourrierec, D.; Ormson, S. M.; Brown, R. G. *Prog. React. Kinet.* **1994**, *19*, 211. (g) Tolbert, L. M.; Solntsev, K. M. *Acc. Chem. Res.* **2002**, *35*, 19. (h) Agmon, N. *J. Phys. Chem. A* **2005**, *109*, 13.
(2) Weller, A. *Z. Elektrochem.* **1956**, *60*, 1144.
(3) (a) Stüber, G. J.; Kieninger, M.; Schettler, H.; Busch, W.; Göller, B.; Frnke, J.; Kramer, H. E. A.; Hoier, H.; Henkel, S.; Fischer, P.; Port, H.; Hirsch, T.; Rytz, G.; Birbaum, J.-L. *J. Phys. Chem.* **1995**, *99*, 10097. (b) Keck, J.; Kramer, H. E. A.; Port, H.; Hirsch, T.; Fischer, P.; Rytz, G. *J. Phys. Chem.* **1996**, *100*, 14468.
(4) (a) Chou, P.-T.; McMorrow, D.; Aartsma, T. J.; Kasha, M. *J. Phys. Chem.* **1984**, *88*, 4596. (b) Parthenopoulos, D. A.; McMorrow, D. P.; Kasha, M. *J. Phys. Chem.* **1991**, *95*, 2668. (c) Kasha, M. *Acta Phys. Pol.* **1987**, *71A*, 717. (d) Park, S.; Kwon, O.-H.; Kim, S.; Park, S.; Choi, M.-G.; Cha, M.; Park, S. Y.; Jang, D.-J. *J. Am. Chem. Soc.* **2005**, *127*, 10070.
(5) Pla-Dalmau, A.; Bross, A. D. *Mater. Res. Symp. Proc.* **1994**, *148*, 163.
(6) Vollmer, F.; Rettig, W. *J. Photochem. Photobiol., A* **1996**, *95*, 143.
(7) (a) Lukeman, M.; Wan, P. *J. Am. Chem. Soc.* **2002**, *124*, 9458. (b) Lukeman, M.; Wan, P. *J. Am. Chem. Soc.* **2003**, *125*, 1164. (c) Flegel, M.; Lukeman, M.; Huck, L.; Wan, P. *J. Am. Chem. Soc.* **2004**, *126*, 7890.

10.1021/jo0524728 CCC: $33.50
Published on Web 03/09/2006

trapped by water giving anthracene addition product **6** in relatively high yield (eq 2).[7c]

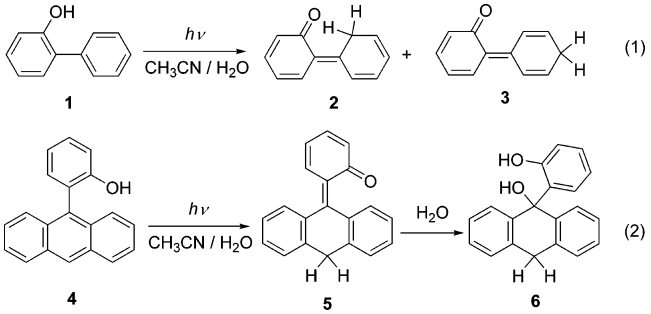

In this study we further explore the potential of ESIPT in other HPA systems. Formation of quinone methides from HPA's is of special interest since it can be facilitated by light of longer wavelengths (350−400 nm), where the anthracene moiety absorbs. Hence, HPA's may find potential use in biological systems (e.g., as DNA alkylating agents[8]), since anthracenes can be excited at sufficiently long wavelengths without interference of absorption of light by most biological molecules. Four new HPA derivatives **7**−**10** were synthesized and their ESIPT

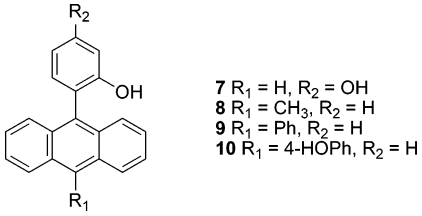

chemistry investigated. Compound **7** is different from the parent anthracene derivative **4**, by bearing an additional electron donating and potentially acidic substituent (OH group). All of HPA derivatives **8**−**10** have a substituent at position 10 of the anthracene ring. This was designed to explore the effect of increased steric hindrance (and extended conjugation in **9** and **10**) on the anticipated ESIPT to position 10. One additional question we wanted to address was whether ESIPT can be directed to two or more different anthracene ring positions.

Results and Discussion

Synthesis. The HPA derivatives **7**−**10** were prepared from the corresponding methoxy compounds (**15**, **16**, **20**, and **22**, respectively) by treatment with BBr_3. The methoxy derivatives were synthesized by Suzuki biaryl coupling reactions and their preparations are summarized in eq 3 and Scheme 1. Suzuki

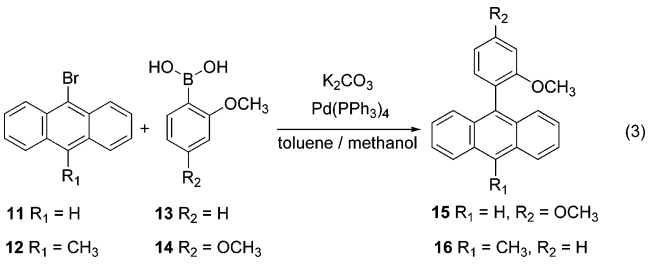

reactions were carried out in toluene/methanol mixture in the presence of K_2CO_3 as base and $Pd(PPh_3)_4$ as catalyst. In some reactions palladium-catalyzed debromination took place, resulting in slightly lower yields of arylated products (formation of **15**, **18**, and **22)**. However, all the couplings were achieved in good to high yields (>60%).

Product Studies. All the HPA derivatives **7**−**10** show typical anthracene absorption with a strong UV−vis absorption band at 250 nm and a weaker but characteristic structured absorption band between 300 and 400 nm. We first examined their photoreactivity by monitoring for changes in the UV−vis absorption spectra upon photolysis. Compounds were irradiated in argon-purged 1:1 H_2O-CH_3OH or H_2O-CH_3CN in UV cuvettes at 350 nm. Photolyses of **7**−**9** were characterized by a decrease in anthracene absorption at all wavelengths (Figure 1a), which was somewhat faster in H_2O-CH_3OH than in H_2O-CH_3CN. If the photolyses were carried out at sufficiently low conversion, the decrease in absorbance was reversible. For example, the recovery of absorbance at 375 nm after photolysis is shown for **9** in 1:1 H_2O-CH_3CN (Figure 1b). The rate of recovery was faster in H_2O-CH_3CN (several minutes) than in H_2O-CH_3OH (>10 min). These observations suggest that photolysis of those HPA's results in formation of anthracene addition products (attack of H_2O or CH_3OH) that are thermally unstable (unlike **6** in eq 2). Under similar photolysis conditions as for **7**−**9**, **10** showed no observable bleaching of UV−vis absorption. This could imply that **10** is photochemicaly inert or that any addition product formed reverts back to starting material very quickly.

To characterize potential irreversibly formed products, preparative irradiations were performed. Thus, on irradiation of HPA derivative **8** in 1:4 H_2O-CH_3CN, products **23**−**25** (Scheme 2) were detected by NMR, formed in ∼20%, ∼10%, and ∼30% yield, respectively, after 4 h of photolysis with ∼50−60% conversion of the starting material. Products **23** and **24** were isolated by TLC on silica gel, while **25** proved to be unstable and readily reverted back to **8**. Although we were not able to isolate hydration products *cis*- and *trans*-**25** in pure form, their structures were assigned according to the characteristic signals present in the ^1H NMR spectrum of the crude photochemical mixture (quartets at δ ∼4.25, doublets at 1.65, and singlets at 9.10 and 10.00 ppm corresponding to the hydrogen bonded phenolic OH protons). Hydration products *cis*- and *trans*-**26** were not detected; they may have been formed but just too reactive for isolation under our conditions. Since **26** is not stabilized by intramolecular hydrogen bonding (as in **25**), it would readily undergo elimination of water giving back starting material.

The structures of isolated compounds **23** and **24** were characterized by NMR. Compound **23** shows in the aliphatic region of three ^1H NMR singlets at δ 5.78, 5.66, and 4.68 ppm in the ratio 2:1:1. There is no signal in ^1H NMR that would correspond to the protons of the methyl group. The aromatic region shows the presence of eight protons, two of which are in the higher field. In the ^{13}C NMR spectrum, there is only one doublet in the aliphatic region at δ 44.6 ppm, while the aromatic region shows eight doublets and a triplet at 110.3 ppm. All the data obtained from NMR point to structure **23** characterized by an exocyclic double bond. Compound **24** is characterized by the presence of two singlets in the aliphatic region of the ^1H NMR spectrum at δ 4.59 and 2.32 ppm (in the ratio 1:3) and the presence of a doublet and a quartet in the ^{13}C NMR at δ

(8) (a) Freccero, M. *Mini-Rev. Org. Chem.* **2004**, *1*, 403. (b) Rietjens, I. M. C. M.; Boersma, M. G.; van der Woude, H.; Jeurissen, S. M. F.; Schutte, M. E.; Alink, G. M. *Mutat. Res.* **2005**, *574*, 124.

SCHEME 1

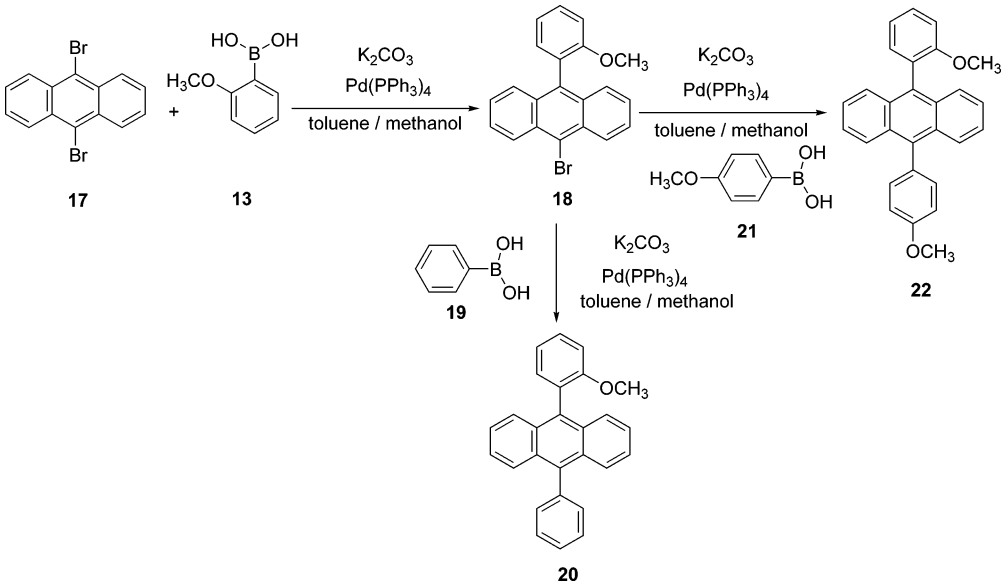

SCHEME 2

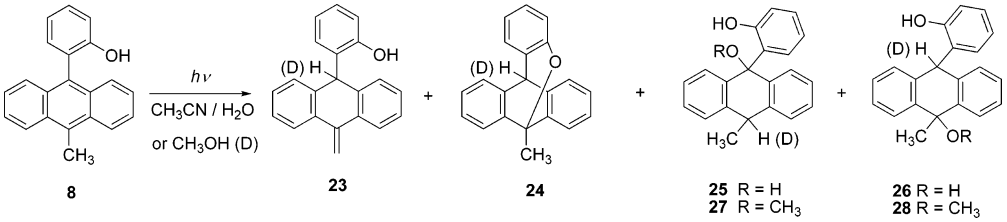

53.0 and 21.7 ppm. The aromatic region of the proton spectrum shows eight protons, four of which are shielded, which is in agreement with the ^{13}C spectrum characterized by eight aromatic doublets. The structure was also characterized by 2D NMR techniques. Thus, in the HMBC spectrum the following important interactions can be seen: C7−H5 and C7−H9 (see Experimental Section and the Supporting Information). The NOESY spectrum showed interactions between the following protons: CH_3−H12, H7−H5, and H7−H9. All of these interactions are in agreement with the proposed bridged structure **24**.

Whereas the hydration product **25** requires the presence of water, it is not clear whether water is needed for the formation of **23** and **24**. Therefore, photolysis of **8** was carried out in neat CH_3CN. After 4 h of irradiation, only starting material (HPA **8**) was recovered; no other product was detectable by NMR or TLC. However, irradiation of **8** in neat CH_3CN in the presence of Bu_4NClO_4 (3 mM) gave **23** as the only product in 10% yield. Compound **24** was not detected; if formed, it may have reverted to **23** in the presence Bu_4NClO_4. In any case, this result shows that a protic solvent is not required for the formation of **23**, but the media has to be sufficiently polar, which can be achieved by either the addition of water or salts. The quantum yield of formation of **23** in 1:4 H_2O−CH_3CN was determined by using a secondary reference (photolysis of **4** in CH_3CN−D_2O giving deuterated **4** and **6**; $\Phi = 0.09$).[7c] In this way, the quantum yield of formation of **23** was estimated to be 0.006, which is about 10 times smaller than the reference reaction. Hydration products **25**, as well as bicyclic compound **24**, are not thermally stabile and readily revert to **8**. Therefore, the amounts of **24** and **25** detected by NMR after photolyses were not reproducible, so their quantum yield of formation is not reported. In addition, for the same reasons as described above, we have not attempted to measure quantum yields for loss of substrate as this is also problematic due to reversion of products back to starting material. Hence, the quantum yield of about 0.006 for formation of **23** may be regarded as a lower limit of overall reactivity of this system.

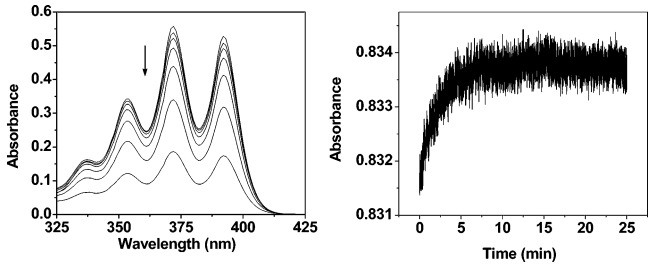

FIGURE 1. (a) Absorption spectra showing loss of the anthracene absorption band on photolysis (350 nm) of HPA **9** in 1:1 CH_3OH−H_2O taken after the following irradiation times: 1, 2, 4, 8, 16, and 32 min. (b) Time dependence of the recovery of absorbance monitored at 375 nm after initial photolysis for HPA **9** (1:1 CH_3CN−H_2O) carried out under low conversion. At higher conversions, the recovery is not as clean due to formation of products that do not revert back to substrate (vide infra) and also some residual photodecomposition.

Preparative irradiations of **8** in CH_3OH were also carried out. Methanol is a better nucleophile than H_2O, so the addition products should be formed with higher efficiency. Additionally, CH_3OH adducts should exhibit higher chemical stability than the corresponding hydration products. After 1 h of photolysis of **8** in neat CH_3OH, there was ∼65% conversion of the starting material and formation of four adducts: *cis*- and *trans*-**27** (∼40%) and *cis*- and *trans*-**28** (∼15%). Besides **27** and **28**,

which were the major products, some smaller amounts of **23** (<10%) and **24** (traces) were also formed (Scheme 2, Table 1). We were not able to isolate **27** and **28** because they readily undergo elimination of methanol on silica, giving starting material. However, evidence of their formation was obtained from the ^{1}H NMR spectra of crude photochemical mixtures. Thus, *cis*- and *trans*-**27** are characterized by the presence of hydrogen-bonded OH signals at δ 10.33 and 10.09 ppm (ratio 1:10), methoxy signals at ∼3 ppm, quartets at ∼4.3 ppm, and doublets at ∼1.65 ppm. On the other hand, *cis*- and *trans*-**28** show in the ^{1}H NMR spectrum triarylmethyl singlets at δ ∼5.7 ppm, methoxy singlets at 2.80 and 2.78 ppm (ratio 1:2), and methyl singlets at ∼1.94 ppm.

To investigate whether products **23**, **24**, **27**, and **28** could be ascribed to initial ESIPT (formal or direct), irradiation of the (methoxyphenyl)anthracene derivative **16** in CH_3OH was carried out. No photoreaction was detected after 1 h of photolysis. This indicates that the phenolic OH group in **8** is required (participates) in the photochemical reaction giving rise to the above products, presumably via a solvent-mediated ESIPT mechanism. Additionally, **8** was also irradiated in CH_3OD. It gave a mixture containing starting material **8** (75%), without any deuterium incorporated in the molecule, and deuterated products **23** (5%), **24** (traces), **27** (15%), and **28** (5%) (Scheme 2, Table 1). Deuterium incorporation in the products was observed from the disappearance of the signals in ^{1}H NMR, comparing to the spectra after photolysis in CH_3OH at δ 5.66, 4.59, 4.30, and 5.70 ppm, respectively. In addition to disappearance of those signals, the doublet at ∼1.6 ppm (from the compound **27**) became a broad singlet. Formation of deuterated products additionally indicates that ESIPT (or solvent-mediated ESIPT) to position 9 or 10 of the anthracene ring is one of the steps in their formation. Moreover, the conversion of the starting material after 1 h of photolysis in CH_3OD was ∼25%; that is about 2.6 times lower than in CH_3OH (Table 1). The lower conversion is in agreement with the slower transfer of deuterium in ESIPT due to an apparent primary isotope effect.

Formation of two types of CH_3OH adducts (regioisomers **27** and **28**), and incorporation of deuterium in the products at position 9 or 10 of the anthracene ring upon photolysis in CH_3OD, indicates the presence of two types of intermediates that are formed in the ESIPT of HPA **8**, the QM **29** and the zwitterion (ZI) **30**. Hydration products **25** and the CH_3OH adducts **27** probably arise by solvent attack of the QM **29**. On the other hand, **23**, **24**, and **28** are probably formed from the ZI **30**, by elimination reaction, intramolecular cyclization, and nucleophillic attack of CH_3OH, respectively. The CH_3OH adducts **27** and **28** are formed in a 3:1 ratio, as revealed by the integration of methoxy singlets in ^{1}H NMR, giving the approximate ratio of the rates of these two ESIPT pathways. Thus, under the employed conditions (irradiation in CH_3OH), long-range ESIPT to position 10 of the anthracene ring giving **29** is about 3 time faster than the short-range ESIPT to position 9 giving **30**.

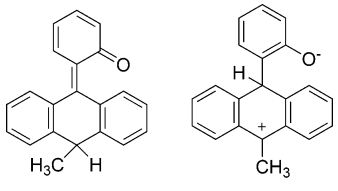

29 **30**

TABLE 1. Relative Yields[a] (%) of the Photochemical Products Formed by Photolysis of 8 in CH_3OH (CH_3OD)

photolysis conditions	8	23	24	27	28
350 nm, 1 h	35	9	1	40	15
350 nm, 1 h[b]	75	5	trace	15	5
300 nm, 2 h	92	1		5	2
254 nm, 2 h	96	1		3	
350 nm, 1 h; 300 nm, 15 min[c]	55	4		27	14
350 nm, 1 h; 254 nm, 15 min[d]	80	3		12	5

[a] Relative yields obtained from the ratio of integrals of signals in ^{1}H NMR ($CDCl_3$). [b] Photolysis carried out in CH_3OD. [c] After 1 h of irradiation at 350 nm, the same solution was then irradiated 15 min at 300 nm. [d] After 1 h of irradiation at 350 nm, the same solution was then irradiated 15 min at 254 nm.

The photochemistry of **8** in CH_3OH was investigated further by changing the irradiation wavelength. The relative yields of the photoproducts obtained from the ^{1}H NMR spectra of the crude mixtures are summarized in Table 1. From the data in Table 1 it can be seen that the highest yields of products were obtained upon photolysis at 350 nm, while irradiation at 300 and 254 nm resulted mostly in recovery of the starting material. This observation can be rationalized by absorption of light (at 300 and 254 nm) by photoproducts which revert to the starting material by a photochemical reaction. After prolonged irradiation, a photostationary state is reached, determined by the ratio of absorption coefficients, and rates of interconversions, of products and the starting material. Thus, after irradiation of **8** at 350 nm where the products are formed with maximal efficiency, subsequent irradiation (of the same solution) at 300 or 254 nm gives back the starting material and hence a lower observed yield of photoproducts (Table 1).

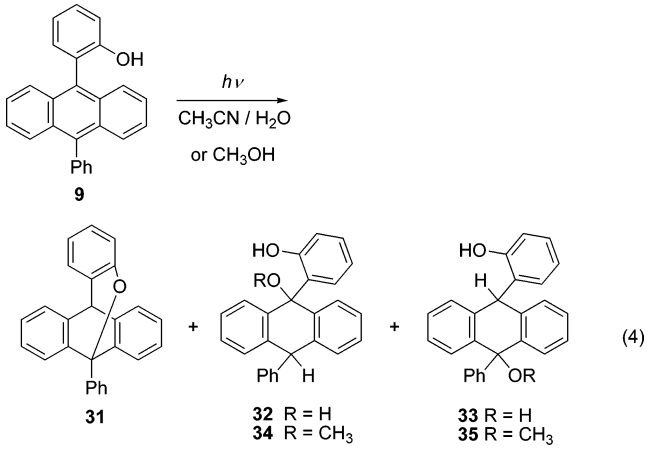

(4)

Photolysis of the HPA derivative **9** in 1:4 H_2O-CH_3CN gave bridged product **31** (eq 4) as the only detectable product, formed in ∼10−20%, after 4 h of irradiation, with ∼20% conversion of the starting material. Compound **31** was isolated by TLC on silica gel and characterized by 1D and 2D NMR. All the NMR data are similar to those for compound **24** and in accordance with the structural characteristics of the bridged structure **31**. Hydration products **32** and **33** were not detected by NMR upon photolysis of **9** in H_2O-CH_3CN. They were probably formed but reverted to the starting material fast enough to avoid detection. To investigate the intriguing possibility that ESIPT might take place to the phenyl ring at the 10 position, **9** was irradiated in 4:1 CH_3CN-D_2O. After 1 h of photolysis, the recovered starting material **9** show no readily detectable exchange by NMR.

For compound **9**, deuterium exchange experiments cannot provide information regarding ESIPT to positions 9 and 10 of the anthracene ring. However, formation of CH_3OH adducts will. After 1 h of irradiation, two CH_3OH adducts were detected by NMR, probably *cis*- and *trans*-**34** (eq 4) which were formed in a 1:1 ratio, in ~40% yield with ~40−50% conversion of the starting material. Any attempt to isolate *cis*- and *trans*-**34** by chromatography resulted in recovery of **9** and isolation of a trace of **31**. The isomers **34** readily undergo elimination of CH_3OH on silica gel giving **9**. However, the presence of *cis*- and *trans*-**34** was indicated from the characteristic signals in the ^1H NMR spectrum of the crude photochemical mixture, corresponding to phenolic OH protons at δ 10.24 and 10.18 ppm, triarylmethyl protons at 5.38 and 5.32 ppm, and methoxy groups at 3.18 and 2.84 ppm. The adducts **35** were not detected by NMR, but they could have been formed but too reactive for isolation. Detection of the CH_3OH adducts **34** and isolation of the bicyclic product **31** confirms that **9** also undergoes ESIPT, giving two types of intermediates (as for **8**): solvent-mediated long-range proton transfer to position 10 of the anthracene ring gives QM **36**, while short-range proton transfer to position 9 gives ZI **37**.

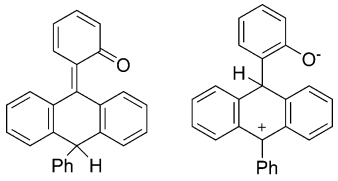

36 **37**

Unlike HPA derivatives **8** and **9**, photolysis of **7** and **10** in CH_3OH or H_2O-CH_3CN (1:4), resulted in only recovery of starting material. We were unable to detect any hydration or CH_3OH addition product by NMR. The explanation probably lies with the fast and efficient elimination of H_2O or CH_3OH from the corresponding adducts. This is in accord with the UV−vis experiments (Figure 1) which showed significantly faster recovery to starting material upon bleaching of the UV−vis absorption of these substrates on photolysis. However, photolysis of **7** in D_2O-CH_3CN (1:4) resulted in deuterium incorporation in the molecule. After 15 min, 23% of the hydrogen at position 10 of the anthracene ring was replaced by deuterium, whereas 1 h of irradiation furnished 60% of deuterated **7**. Formation of deuterated HPA **7** is explained by formaton of QM **38** via ESIPT. The quantum yield of deuterium incorporation in position 10 was estimated by using a secondary reference (photolysis of **4** in CH_3CN-D_2O, giving deuterated **4** and **6**; $\Phi = 0.09$)[7c] that gave a quantum yield of 0.06, which is similar to the efficiency of deuterium incorporation in the parent **4**.

Although we were not able to detect any product upon photolysis of **10** in CH_3CN-H_2O or CH_3OH, in analogy with the ESIPT chemistry observed for **7**−**9**, one might assume that **10** also undergoes this type of photochemistry, resulting in protonation of positions 10 and 9 of the anthracene ring, giving rise to intermediates QM **39** and ZI **40**, respectively. Both **7** and **10** are substituted by a *p*-hydroxyl group on a phenyl ring. Such a group is a well-know electron-donating group in the ground state and may destabilize any addition products that may be formed in these systems, thus making them much prone to decomposition (reversion back to substrate). This is already indicated by the above results for **7**; we can assume with some confidence that it is operating to full effectiveness for **10**.

TABLE 2. Photophysical Characteristics of the HPA Derivatives 7−10[a]

compd	λ_{abs} (nm)[b]	λ_{fl} (nm)[c]	Φ_f[d]	τ[e] (ns)
7	254, 346, 365, 384	420	0.27	3.7
8	258, 355, 374, 394	402, 423, 445 (sh), 475 (sh)	0.62	11.3
9	258, 354, 372, 392	405, 425, 450 (sh)	0.93	8.7
10	259, 355, 373, 393	416, 430 (sh)	0.64	4.2

[a] Measurements were performed in CH_3CN at 20 °C. [b] Maxima in the absorption spectra. [c] Maxima in the fluorescence spectra. [d] Fluorescence quantum yield measured relative to quinine sulfate in 1.0 N H_2SO_4 ($\Phi_{fl} = 0.55$).[10] Estimated error is ±0.05. [e] Singlet excited-state lifetime, measured by single photon counting, estimated error ±0.1 ns.

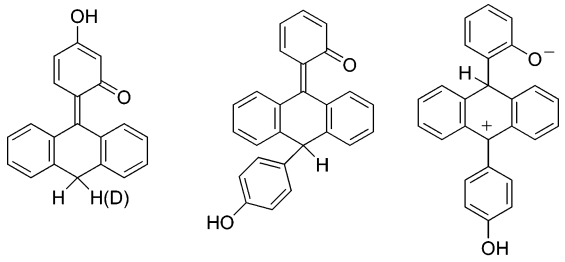

38 **39** **40**

Fluorescence Measurements. All the HPA derivatives **7**−**10** were characterized by relatively strong fluorescence emission in CH_3CN with bands between 400 and 500 nm, typical for anthracene fluorescence (Table 2). Stokes shifts for all the compounds were relatively small indicating that there is only a small perturbation of the geometry for the fluorescent state. The fluorescence of **7** was the most perturbed from classical anthracene emission. It was structureless and characterized by a lower quantum yield of fluorescence compared to **4** ($\Phi_f = 0.50$, $\tau = 5.9$ ns).[7c] The introduction of a methyl substituent at the 10 position in **8** resulted in an increase of the fluorescence quantum yield and lifetime, contrary to expectation. However, the singlet lifetime and emission spectrum of **9** are similar to those reported for other diphenylanthracenes (~8 ns).[9] From fluorescence and UV−vis spectra of **7**−**10** we may conclude that these compounds are characterized by weak conjugation (interaction) between the anthracene and phenol moieties in both ground and excited singlet states.

The fluorescence emissions of all the HPA's are quenched upon addition of water. One example of quenching by water is shown in Figure 2 for the derivative **10**. The quenching (for all the HPA's **7**−**10**) is characterized by a decrease of the fluorescence intensity without any shift of the maxima. New bands that might arise from emission of phenolates were not detected, indicating that water quenching is due to solvent-mediated ESIPT (giving rise to intermediate QM's and ZI's), rather than simply proton transfer to the solvent (giving excited state phenolates). That fact that fluorescence from phenolates was not observed does not rule out their formation. They may be formed but are very short lived (i.e., very reactive). For example, the excited state phenolate may undergo protonation of the anthracene at the 9 or 10 positions giving the observed

(9) (a) Schoof, S.; Guesten, H.; Von Sonntag, C. *Ber. Bunsen-Ges.* **1978**, *82*, 1068. (b) Meech, S. R.; Phillips, D. *J. Photochem.* **1983**, *23*, 193.

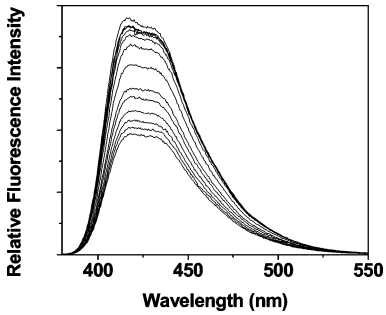

FIGURE 2. Quenching of the fluorescence of HPA **10** in CH_3CN (λ_{ex} = 375 nm) by addition of water ([H_2O] ranging from 0 to 10 M).

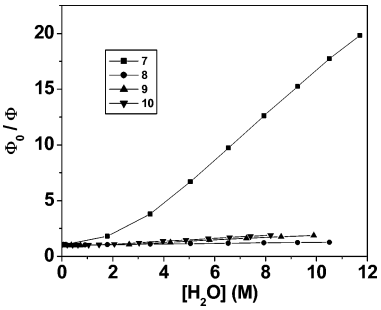

FIGURE 3. Stern−Volmer plots of fluorescence quenching vs water concentration for HPA's **7**−**10** (in CH_3CN).

photochemistry reported above. Nevertheless, this pathway may still be regarded as a formal ESIPT mechanism. In general, however, excited state proton transfer to solvent requires much higher water content for most phenols. The observation of fluorescence quenching at relatively low water content as observed in these phenol systems would suggest that a different water-mediated quenching pathway is operative, viz., a water-mediated ESIPT to the anthracene 9 and 10 positions.

Stern−Volmer plots (Figure 3) show nonlinear dependence of the quenching efficiency on water concentration. With a small amount of water (up to 5 M) quenching could be described as a polynomial function, which is in agreement with a transfer of proton to clusters of water molecules, seen in similar water-mediated ESIPT systems.[11] Water quenching is the most efficient for the HPA derivative **7** (∼10 times more efficient than for HPA's **8**−**10**). Relatively lower quenching efficiencies for **8**−**10** indicate lower quantum yields of their water-mediated ESIPT reactions. However, considering the high quantum yields of fluorescence, especially for HPA's **8** and **9**, ESIPT is a quite important nonradiative deactivation pathway from the singlet excited state.

Nanosecond Laser Flash Photolysis. Nanosecond LFP was used to probe for transient intermediates, viz., QM's (**29**, **36**, **38**, and **39**) and ZI's, (**30**, **37**, and **40**) formed by ESIPT in HPA's **7**−**10** (Scheme 3). Transient absorption spectra were recorded in 1:1 CH_3CN-H_2O, where the formation of the intermediates was anticipated, and in neat CH_3CN, which was the control run (where the intermediates are not formed, based on product studies). The transient absorption spectra for all compounds (in both solvents) were characterized by strong transient absorptions in the 250−350 nm region that were not affected by oxygen, and negative signals (bleaching) in the 350−400 nm region due to the absorption of the laser flash by the substrate. The bleaching signals for all the derivatives recovered almost completely to baseline indicating good reversibility of the processes initiated by the laser flash. In addition to these bands, the anthracene triplet−triplet absorption was detected. It was significantly influenced (shorter lifetimes) by the presence of oxygen and situated with the maximum at ∼430 nm, in agreement with the literature.[12]

In both solvents, we also detected transient absorptions at longer wavelengths (500−700 nm), where the absorption of QM's was anticipated. Those bands were not affected by the presence of oxygen and were especially pronounced for the HPA's **8** and **9.** However, we observed similar transient absorptions for the (nonreactive) methoxy compound **16**. Decreasing the laser power resulted in higher relative signal intensity at 430 nm compared to the signals in the 500−700 nm region. This suggests that the 500−700 nm transient arises via a two-photon process (possibly forming radical cations). Addition of ethanolamine, a known QM quencher,[13] resulted in no observable changes in any of the observed transients obtained for **7** (in CH_3CN-H_2O). We conclude that none of the observed transient absorptions correspond to QM's. Although QM's are probably formed as transients, they are probably too weak to be observed in these systems that also have strong bleaching signals and triplet−triplet absorptions as well as transients that arise via two-photon processes. Attempts were also made to characterize ZI intermediates **30**, **37**, and **40**. LFP studies were carried out in trifluoroethanol, a polar but less nucleophilic solvent, with the expectation that the transient if formed would be longer lived. However, no detectable transients were observed in the 450−500 nm region where di- or triarylmethyl carbocations are known to absorb.[14] Thus, the proposed ZI's are characterized by short lifetimes, which in addition to their low quantum yields of formation would make their detection very difficult.

Mechanisms of Reaction. Upon excitation with near-visible light, all of the HPA's **7**−**9** (and probably **10** also) undergo formal ESIPT in CH_3CN-H_2O or CH_3OH. Singlet state reactivity has been inferred and is in accord with previous results of related systems.[7] For HPA **7**, only one ESIPT pathway was observed, protonation of the 10 position of the anthracene ring, giving QM **38** (Scheme 3). Short-range ESIPT to position 9 was not observed as this would be intrinsically less favored in the formation of a ZI rather than a neutral and fully conjugated QM. In addition to reverting back to **7** via tautomerization (with deuterium incorporation at the 10 position if carried out in deuterated solvents), QM **38** can react with solvent, giving addition products **41** and **42**.

One of the results that we concluded from our fluorescence data (vide supra) was that there is very little interaction between the phenyl and the anthracene chromophores in ground and excited singlet states of these compounds. However, it is clear that formation of a QM intermediate requires the phenyl and

(10) Olmsted, J. *J. Phys. Chem.* **1979**, *83*, 2581.
(11) (a) Fischer, M.; Wan, P. *J. Am. Chem. Soc.* **1998**, *120*, 2680. (b) Fischer, M.; Wan, P. *J. Am. Chem. Soc.* **1999**, *121*, 4555.
(12) Carmichael, I.; Helman, W. P.; Hug, G. L. *J. Phys. Chem. Ref. Data* **1987**, *16*, 239.
(13) (a) Brousmiche, D. W.; Wan, P. *J. Photochem. Photobiol., A* **2002**, *149*, 71. (b) Brousmiche, D. W.; Xu, M.; Lukeman, M.; Wan, P. *J. Am. Chem. Soc.* **2003**, *125*, 12961. (c) Lukeman, M.; Veale, D.; Wan, P.; Munasinghe, V. R. N.; Corrie, J. E. T. *Can. J. Chem.* **2004**, *82*, 240.
(14) (a) McClelland, R. A.; Kanagasabapathy, V. M.; Banait, N. S.; Steenken, S. *J. Am. Chem. Soc.* **1989**, *111*, 3966. (b) Cozens, F. L.; Kanagasabaphaty, V. M.; McClelland, R. A.; Steenken, S. *Can. J. Chem.* **1999**, *77*, 2069.

SCHEME 3

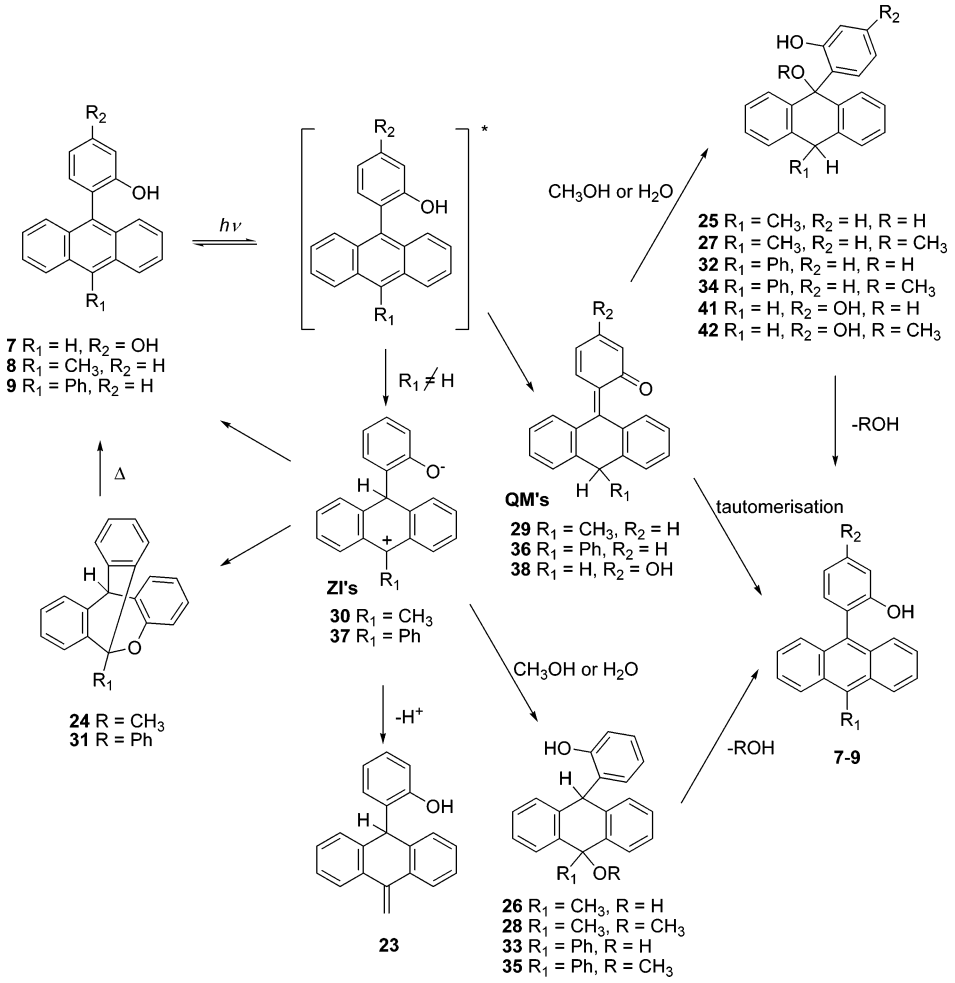

anthracene rings to interact better, to give a more conjugated system as implied in the QM structure. The formation of ZI's may also require enhanced electronic communication between these rings to facilitate the transfer of the proton although it may be somewhat less in this case. That is, how and when is the proton transferred and how is it coupled with the required torsional motion between the phenyl and anthracenyl moieties? We have no way of directly probing these events, but in a previous paper,[7c] several possible pathways were delineated that will not be repeated here.

Substitution of the anthracene ring at position 10 with a simple methyl group or a phenyl group (derivatives **8** and **9**, respectively) results in an overall decrease in ESIPT efficiency that may be attributable to a simple steric effect as well as observation of a new ESIPT pathway: short-range ESIPT to the 9 position. The overall decrease in ESIPT efficiency was manifested in lower efficiencies of fluorescence quenching by water. ESIPT to the 10 position gives rise to QMs **29** and **36** which may be trapped by solvent. However, in these systems, a short-range ESIPT operates to give ZI's **30** and **37**. This ESIPT may be the direct proton-transfer pathway since it operates even in neat CH_3CN with added Bu_4NClO_4 (vide supra). The operation of this pathway may be simply rationalized as the result of steric congestion imposed at the 10 position on adding a methyl or a phenyl group.

Both ZI and QM intermediates may revert back to starting material or be trapped by solvents (H_2O or CH_3OH) giving a variety of addition products (**25**−**28**, **32**−**35**). The ZI intermediates also react by intramolecular ring closure giving bridged products **24** and **31**, and also undergo elimination (feasible with the methyl derivative **30**) giving exocyclic alkene **23**. The relative yield of CH_3OH adducts **27** and **28** formed by ESIPT of HPA **8** (under conditions where formation of **23** and **24** is negligible) gives the approximate ratio of the rates of the two competing ESIPT pathways. In neat CH_3OH, long-range ESIPT to position 10 of the anthracene ring is about 3 times faster than the short-range ESIPT to position 9. Thus, we anticipate then that in the case where the methyl group is removed, the long-range ESIPT pathway should dominate, as it does in the case of **7** and **4**.

Finally, these results amply demonstrate that the overall chemistry in ESIPT from phenol to the anthracene moiety in these compounds is highly sensitive to structural changes in the chromophore. It is possible to have a totally reversible process in which no products are isolable or it can result in the formation of numerous interesting anthracene addition or rearrangement products. The formation of ZI's was shown to occur via a pathway that was not initially anticipated but may ultimately be useful for preparing bridged dibenzooxepines. To the best of our knowledge there were only two reports for the preparation of such a ring system.[15]

(15) (a) Mori, A.; Kawakami, H.; Kato, N.; Wu, S.-P.; Takeshita, H. *Org. Biomol. Chem.* **2003**, *1*, 1730. (b) Mori, A.; Yokoo, H.; Hatsui, T. *Tetrahedron* **2004**, *60*, 8783.

Experimental Section

Suzuki Reaction: General Procedure. A solution of 1 equiv of bromo compound in toluene was added to a methanol solution of 1 equiv of boronic acid. To the reaction mixture was added 2 equiv of potassium carbonate and the solution was purged with N_2. To the reaction mixture was added 0.01−0.02 equiv of Pd-$(PPh_3)_4$ and the solution was purged again with N_2. The reaction mixture was heated at reflux temperature for 24 h under N_2. To the cooled reaction mixture was added water and extractions with CH_2Cl_2 were carried out. Collected extracts were dried over anhydrous $MgSO_4$, solvent was evaporated, and the residue was chromatographed on a column of silica gel with hexane/CH_2Cl_2 mixture as eluent.

9-Bromo-10-(2′-methoxyphenyl)anthracene (18). Starting from 1.00 g (6.6 mmol) of 2-methoxyphenyl boronic acid (**13**) and 2.21 g (6.6 mmol) 9,10-dibromoanthracene (**17**) the reaction furnished 1.46 g (60.9%) of product **18**.

Yellow crystals, mp 135−136 °C; ^{1}H NMR ($CDCl_3$, 300 MHz) δ 8.48 (d, 2H, J = 8.8 Hz), 7.50 (d, 2H, J = 8.8 Hz), 7.38−7.48 (m, 3H), 7.23 (ddd, 2H, J = 1.5 Hz, J = 6.6 Hz, J = 8.8 Hz), 7.12 (dd, 1H, J = 2.2 Hz, J = 7.4 Hz), 7.05 (ddd, 1H, J = 2.2 Hz, J = 7.4 Hz, J = 7.4 Hz), 7.00 (d, 1H, J = 8.1 Hz), 3.46 (s, 3H); ^{13}C NMR ($CDCl_3$, 75 MHz) δ 158.2, 135.0, 133.0, 131.5, 130.7, 130.0, 128.2, 127.6, 127.2, 125.8, 123.1, 121.1, 111.6, 56.0, one singlet was not seen; MS (EI) *m*/*z* 365 (M^+, 30), 364 (M^+, 100), 363 (M^+, 30), 362 (M^+, 100), 268 (50), 239 (40); HRMS, calculated for $C_{21}H_{15}BrO$ 362.0306, observed 362.0305.

9-(2′,4′-Dimethoxyphenyl)anthracene (15). Starting from 706 mg (2.75 mmol) of 9-bromoanthracene (**11**) and 500 mg (2.75 mmol) of 2,4-dimethoxyphenyl boronic acid (**14**) the reaction furnished 470 mg (54.3%) of product **15**.

Colorless crystals, mp 228−229 °C; ^{1}H NMR ($CDCl_3$, 300 MHz) δ 8.46 (s, 1H), 8.01 (d, 2H, J = 8.8 Hz), 7.64 (d, 2H, J = 8.8 Hz), 7.43 (dd, 2H, J = 6.6 Hz, J = 8.8 Hz), 7.32 (dd, 2H, J = 6.6 Hz, J = 8.8 Hz), 7.15 (d, 1H, J = 8.1 Hz), 6.71 (d, 1H, J = 2.2 Hz), 6.69 (dd, 1H, J = 2.2 Hz, J = 8.1 Hz), 3.94 (s, 3H), 3.58 (s, 3H); ^{13}C NMR ($CDCl_3$, 75 MHz) δ 161.0, 159.2, 133.9, 133.4, 131.7, 131.0, 128.6, 127.1, 126.6, 125.3, 125.2, 120.0, 109.8, 104.8, 99.2, 55.9, 55.7; MS (EI) *m*/*z* 315 (M^+, 30), 314 (M^+, 100), 255 (10), 226 (10); HRMS, calculated for $C_{22}H_{18}O_2$ 314.1307, observed 314.1308.

9-(2′-Methoxyphenyl)-10-methylanthracene (16). Starting from 1.75 g (6.5 mmol) of 9-bromo-10-methylanthracene (**12**)[16] and 0.98 g (6.5 mmol) of 2-methoxyphenyl boronic acid (**13**), the reaction furnished 1.73 g (89.2%) of product **16**.

Colorless crystals, mp 150−151 °C; ^{1}H NMR ($CDCl_3$, 300 MHz) δ 8.33 (d, 2H, J = 8.8 Hz), 7.60 (d, 2H, J = 8.8 Hz), 7.52 (ddd, 1H J = 1.5 Hz, J = 7.5 Hz, J = 8.1 Hz), 7.48 (dd, 2H, J = 6.6 Hz, J = 8.8 Hz), 7.31 (dd, 2H, J = 6.6 Hz, J = 8.8 Hz), 7.23 (dd, 1H, J = 1.5 Hz, J = 7.4 Hz), 7.15 (dd, 1H, J = 7.4 Hz, J = 7.5 Hz), 7.13 (d, 1H, J = 8.1 Hz), 3.60 (s, 3H), 3.16 (s, 3H); ^{13}C NMR ($CDCl_3$, 75 MHz) δ 158.3, 133.3, 130.3, 130.2, 129.4, 128.0, 127.7, 125.1, 125.0, 124.9, 120.9, 111.4, 55.9, 14.4, one singlet was not seen; MS (EI) *m*/*z* 299 (M^+, 30), 298 (M^+, 100), 268 (30); HRMS calculated for $C_{22}H_{18}O$ 298.1358, observed 298.1358.

9-(2′-Methoxyphenyl)-10-phenylanthracene (20). Starting from 400 mg (1.10 mmol) of 9-bromo-10-(2′-methoxyphenyl)anthracene (**18**) and 150 mg (1.21 mmol) of phenyl boronic acid (**19**), the reaction furnished 390 mg (98.5%) of product **20**.

Colorless crystals, mp 222−223 °C; ^{1}H NMR ($CDCl_3$, 500 MHz) δ 7.65−7.79 (m, 2H), 7.60−7.64 (m, 2H), 7.56−7.60 (m, 2H), 7.49−7.56 (m, 3H), 7.45 (dd, 1H, J = 2.2 Hz, J = 7.4 Hz), 7.25−7.31 (m, 5H), 7.17 (dd, 1H, J = 1.1 Hz, J = 7.3 Hz), 7.16 (dd, 1H, J = 7.3 Hz, J = 7.8 Hz) 3.65 (s, 3H); ^{13}C NMR ($CDCl_3$, 75 MHz) δ 158.3, 139.4, 137.2, 134.0, 133.2, 131.64, 131.60, 130.2, 129.5, 128.6, 127.8, 127.6, 127.3, 127.1, 125.1, 121.0, 111.5, one singlet was not seen; MS (EI) *m*/*z* 360 (M^+, 10), 284 (100), 278 (50), 277 (100), 268 (30); HRMS calculated for $C_{27}H_{20}O$ 360.1514, observed 360.1513.

9-(2′-Methoxyphenyl)-10-(4′-methoxyphenyl)anthracene (22). Starting from 500 mg (1.10 mmol) of 9-bromo-10-(2′-methoxyphenyl)anthracene (**18**) and 230 mg (1.51 mmol) of 4-methoxyphenyl boronic acid (**21**), the reaction furnished 370 mg (68.7%) of product **22**.

Colorless crystals, mp 208−209 °C; ^{1}H NMR ($CDCl_3$, 300 MHz) δ 7.68−7.78 (m, 2H), 7.58−7.66 (m, 2H), 7.54 (dd, 1H, J = 2.2 Hz, J = 8.1 Hz), 7.45 (dd, 2H, J = 6.6 Hz, J = 9.5 Hz), 7.26−7.33 (m, 5H), 7.10−7.20 (m, 4H), 3.95 (s, 3H), 3.64 (s, 3H); ^{13}C NMR ($CDCl_3$, 75 MHz) δ 159.2, 158.3, 137.0, 133.9, 133.2, 132.70, 132.66, 131.5, 130.6, 130.3, 129.5, 127.9, 127.3, 127.1, 125.1, 125.0, 121.0, 114.0, 111.5, 56.0, 55.6, one doublet more due to not equivalent carbons; MS (EI) *m*/*z* 391 (M^+, 30), 390 (M^+, 100), 321 (20), 97 (20), 83 (20); HRMS calculated for $C_{28}H_{22}O_2$ 390.1620, observed 390.1621.

Cleavage of the Methyl Group by Use of BBr_3: General Procedure. The methoxy compound was dissolved in dichloromethane and the solution was cooled to 0 °C with an ice-water bath. By use of a syringe a dichloromethane solution (1M) of 5 equiv of BBr_3 per equiv of methoxy substituent was added dropwise under nitrogen. The ice bath was removed and the reaction mixture was stirred at room temperature for an additional 2 h under nitrogen. Reaction was quenched by addition of water and the layers were separated. The water layer was extracted two more times with use of CH_2Cl_2. Combined extracts were dried over anhydrous $MgSO_4$, solvent was removed, and the residue was chromatographed on a column of silica gel with hexane/CH_2Cl_2 as eluent.

9-(2′,4′-Dihydroxyphenyl)anthracene (7). Starting from 540 mg (1.72 mmol) of 9-(2′,4′-dimethoxyphenyl)anthracene (**15**), the reaction furnished 480 mg (97.5%) of product **7**.

Yellow crystals, mp 161−162 °C; ^{1}H NMR ($CDCl_3$, 300 MHz) δ 8.53 (s, 1H), 8.04 (d, 2H, J = 8.0 Hz), 7.70 (d, 2H, J = 8.8 Hz), 7.48 (dd, 2H, J = 6.6 Hz, J = 8.0 Hz), 7.40 (dd, 2H, J = 6.6 Hz, J = 8.8 Hz), 7.09 (d, 1H, J = 8.1 Hz), 6.65 (d, 1H, J = 2.2 Hz), 6.62 (dd, 1H, J = 2.2 Hz, J = 8.1 Hz), 5.03 (s, 1H, OH), 4.53 (s, 1H, OH); ^{13}C NMR ($CDCl_3$, 75 MHz) δ 157.2, 155.0, 133.1, 131.8, 131.5, 129.6, 128.8, 128.2, 126.6, 126.3, 125.8, 116.8, 108.4, 103.0; MS (EI) *m*/*z* 287 (M^+, 21), 286 (M^+, 100), 202 (10), 119 (10); HRMS calculated for $C_{20}H_{14}O_2$ 286.0994, observed 286.0997.

9-(2′-Hydroxyphenyl)-10-methylanthracene (8). Starting from 1.40 g (4.70 mmol) of 9-(2′-methoxyphenyl)-10-methylanthracene (**16**), the reaction furnished 1.33 g (99%) of product **8**.

Yellow crystals, mp 134−135 °C; ^{1}H NMR ($CDCl_3$, 300 MHz) δ 8.38 (d, 2H, J = 8.8 Hz), 7.67 (d, 2H, J = 8.8 Hz), 7.53 (dd, 2H, J = 6.6 Hz, J = 8.8 Hz), 7.46 (ddd, 1H J = 1.5 Hz, J = 7.5 Hz, J = 8.1 Hz), 7.40 (dd, 2H, J = 6.6 Hz, J = 8.8 Hz), 7.24 (dd, 1H, J = 1.5 Hz, J = 7.4 Hz), 7.15 (d, 1H, J = 8.1 Hz), 7.13 (dd, 1H, J = 7.4 Hz, J = 7.5 Hz), 4.50 (s, 1H, OH), 3.19 (s, 3H); ^{13}C NMR ($CDCl_3$, 75 MHz) δ 154.1, 132.6, 132.2, 130.8, 130.3, 130.0, 128.3, 127.0, 126.0, 125.7, 125.2, 124.7, 120.9, 115.8, 14.5; MS (EI) *m*/*z* 285 (M^+, 25), 284 (M^+, 100), 268 (20), 239 (20); HRMS calculated for $C_{21}H_{16}O$ 284.1201, observed 284.1203.

9-(2′-Hydroxyphenyl)-10-phenylanthracene (9). Starting from 550 mg (1.53 mmol) of 9-(2-methoxyphenyl)-10-phenylanthracene (**20**), the reaction furnished 510 mg (96.4%) of product **9**.

Yellow crystals, mp 212−213 °C; ^{1}H NMR ($CDCl_3$, 500 MHz) δ 7.68−7.72 (m, 4H), 7.58−7.62 (m, 2H), 7.55 (tt, 1H, J = 1.5 Hz, J = 7.3 Hz), 7.44−7.51 (m, 3H), 7.33−7.40 (m, 4H), 7.30 (dd, 1H, J = 1.8 Hz, J = 7.5 Hz), 7.18 (dd, 1H, J = 1.1 Hz, J = 8.1 Hz), 7.16 (ddd, 1H, J = 1.1 Hz, J = 7.3 Hz, J = 7.5 Hz), 4.59 (s, 1H, OH); ^{13}C NMR ($CDCl_3$, 75 MHz) δ 154.1, 138.89, 138.86, 132.5, 131.4, 131.3, 130.8, 130.4, 130.1, 129.9, 128.7, 127.9, 127.6, 126.34, 126.27, 125.6, 124.5, 121.0, 116.0, one doublet more due to not equivalent carbons; MS (EI) *m*/*z* 347 (M^+, 28), 346 (M^+,

(16) Duan, S.; Turk, J.; Speigle, J.; Corbin, J.; Masnovi, J.; Baker, R. J. *J. Org. Chem.* **2000**, *65*, 3005.

100), 252 (10), 206 (10), 163 (10); HRMS calculated for $C_{26}H_{18}O$ 346.1358, observed 346.1359.

9-(2′-Hydroxyphenyl)-10-(4′-hydroxyphenyl)anthracene (10). Starting from 350 mg (0.90 mmol) of 9-(2′-methoxyphenyl)-10-(4′-methoxyphenyl)anthracene (**22**), the reaction furnished 310 mg (95.4%) of product **10**.

Yellow crystals, mp 260−261 °C decomposition; ^{1}H NMR (acetone-d_6, 300 MHz) δ 8.66 (s, 1H, OH), 7.97 (s, 1H, OH), 7.68−7.80 (m, 4H), 7.46 (ddd, 1H, J = 1.5 Hz, J = 7.3 Hz, J = 8.1 Hz), 7.33−7.40 (m, 4H), 7.22−7.33 (m, 3H), 7.20 (d, 1H, J = 8.1 Hz), 7.15 (d, 2H, J = 8.8 Hz), 7.12 (dd, 1H, J = 7.3 Hz, J = 7.4 Hz); ^{13}C NMR (acetone-d_6, 75 MHz) δ 158.0, 156.6, 138.2, 134.3, 133.6, 133.3, 133.2, 131.42, 131.38, 130.6, 130.4, 127.9, 127.8, 126.2, 126.0, 125.9, 120.8, 117.0, 116.41, 116.39; MS (EI) *m*/*z* 363 (M^+, 30), 362 (M^+, 100), 268 (10); HRMS calculated for $C_{26}H_{18}O_2$ 362.1307, observed 362.1307.

Preparative Irradiation Experiments: General Procedure. A 100 mL sample of the solution (4:1 CH_3CN-H_2O) containing typically 100 mg of the HPA ($c \sim 10^{-3}$ M) was purged with argon for 15 min and irradiated 1 to 4 h at 350 nm in a Rayonet reactor. During irradiation, solution was continuously purged with argon and cooled by water. After irradiation, extractions with CH_2Cl_2 were carried out, the extracts were dried over anhydrous $MgSO_4$, solvent was evaporated, and the residue was chromatographed on a thin layer of silica (TLC) with hexane/CH_2Cl_2 mixture as eluent.

Photolysis of 9-(2′-Hydroxyphenyl)-10-methylanthracene (8). A 100 mL sample of the 4:1 CH_3CN-H_2O solution, containing 150 mg of the HPA **8**, was irradiated 4 h at 350 nm. From TLC with a hexane/CH_2Cl_2 (1:1) mixture the following compounds were isolated: 30 mg (20%) of the starting material, 8 mg (5.3%) of the bicyclic product 6-methyl-6,11-(1,2-phenyleno)-6,11-dihydro[*b*,*e*]-dibenzooxepine (**24**), and 30 mg (20%) of the vinyl product 2-(10-methylene-9,10-dihydroanthracen-9-yl)phenol (**23**).

2-(10-Methylene-9,10-dihydroanthracen-9-yl)phenol (**23**): yellow

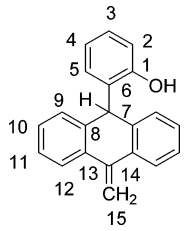

crystals, mp 92−94 °C; ^{1}H NMR ($CDCl_3$, 300 MHz) δ 7.76 (d, 2H, J = 8.8 Hz, H-12), 7.18−7.31 (m, 6H), 7.06 (ddd, 1H, J = 1.5 Hz, J = 7.4 Hz, J = 8.1 Hz, H-3), 6.97 (dd, 1H, J = 1.5 Hz, J = 8.1 Hz, H-5), 6.81 (d, 1H, J = 8.1 Hz, H-2), 6.77 (dd, 1H, J = 7.4 Hz, J = 8.1 Hz, H-4), 5.78 (s, 2H, H-15), 5.66 (s, 1H, H-7), 4.68 (s, 1H, OH); ^{13}C NMR ($CDCl_3$, 75 MHz) δ 152.8 (s, C-1), 141.7 (s, C-14), 137.6 (s), 135.2 (s), 131.1 (s), 131.0 (d, C-5), 128.4 (d), 128.3 (d), 128.1 (d, C-3), 127.2 (d), 124.5 (d), 121.5 (d, C-4), 116.5 (d, C-2), 110.3 (t, C-15), 44.6 (d, C-7); MS (EI) *m*/*z* 285 (M^+, 25), 284 (M^+, 100), 268 (10), 191 (10); HRMS calculated for $C_{21}H_{16}O$ 284.1201, observed 284.1201.

6-Methyl-6,11-(1,2-phenyleno)-6,11-dihydro-[*b*,*e*]dibenzooxepine (**24**): colorless crystals, thermally unstable, rearranges to 9-(2′-

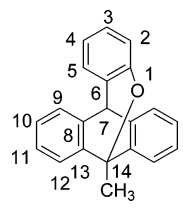

hydroxyphenyl)-10-methylanthracene (**8**) (mp 134−135 °C); ^{1}H NMR ($CDCl_3$, 500 MHz) δ 7.60 (dd, 2H, J = 1.5 Hz, J = 7.4 Hz, H-12), 7.36 (dd, 2H, J = 1.5 Hz, J = 7.4 Hz, H-9), 7.26 (ddd, 2H, J = 1.5 Hz, J = 7.3 Hz, J = 7.4 Hz, H-11), 7.22 (ddd, 2H, J = 1.5 Hz, J = 7.3 Hz, J = 7.4 Hz, H-10), 7.16 (dd, 1H, J = 1.5 Hz, J = 7.5 Hz, H-5), 6.98 (ddd, 1H, J = 1.5 Hz, J = 7.3 Hz, J = 8.1 Hz, H-3), 6.71 (ddd, 1H, J = 1.1 Hz, J = 7.3 Hz, J = 7.5 Hz, H-4), 6.54 (dd, 1H, J = 1.1 Hz, J = 8.1 Hz, H-2), 4.59 (s, 1H, H-7), 2.32 (s, 3H, CH_3); ^{13}C NMR ($CDCl_3$, 125 MHz) δ 154.0 (s, C-1), 144.4 (s, C-8), 137.4 (s, C-13), 128.9 (d, C-3), 128.6 (d, C-10), 127.21 (d, C-5), 127.17 (d, C-11), 126.8 (s, C-6), 124.8 (d, C-9), 124.2 (d, C-12), 120.4 (d, C-4), 119.7 (d, C-2), 53.0 (d, C-7), 21.7 (q), signal of C-14, covered by $CDCl_3$;

Photolysis of 9-(2′-Hydroxyphenyl)-10-phenylanthracene (9). A 100 mL sample of the 4:1 CH_3CN-H_2O solution, containing 100 mg of the HPA derivative **9**, was irradiated 4 h at 350 nm. From the TLC with a hexane/CH_2Cl_2 (1:1) mixture the following compounds were isolated: 70 mg (70%) of the starting material and 2.6 mg (2.6%) of the bicyclic product 6-phenyl-6,11-(1,2-phenyleno)-6,11-dihydro-[*b*,*e*]dibenzooxepine (**31**).

6-Phenyl-6,11-(1,2-phenyleno)-6,11-dihydro-[*b*,*e*]dibenzooxepine (**31**): yellow crystals, mp 244−245 °C decomposition; ^{1}H

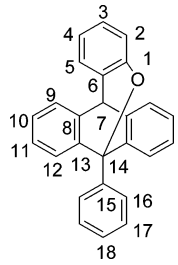

NMR ($CDCl_3$, 500 MHz) δ 8.38 (d, 1H, J = 7.8 Hz, H-16), 7.64 (dd, 1H, J = 7.4 Hz, J = 7.8 Hz, H-17), 7.48 (tt, 1H, J = 1.3 Hz, J = 7.4 Hz, H-18), 7.42 (dd, 1H, J = 7.4 Hz, J = 7.8 Hz, H-17), 7.39 (dd, 2H, J = 1.5 Hz, J = 7.3 Hz, H-9), 7.21 (ddd, J = 1.5 Hz, J = 7.3 Hz, J = 7.4 Hz, H-11), 7.18 (dd, 1H, J = 1.8 Hz, J = 7.5 Hz, H-5), 7.10 (d, 1H, J = 7.8 Hz, H-16), 7.09 (ddd, 2H, J = 1.5 Hz, J = 7.3 Hz, J = 7.8 Hz, H-10), 7.04 (ddd, 1H, J = 1.8 Hz, J = 7.3 Hz, J = 8.1 Hz, H-3), 6.84 (dd, 1H, J = 1.3 Hz, J = 7.8 Hz, H-12), 6.78 (dd, 1H, J = 1.1 Hz, J = 8.1 Hz, H-2), 6.74 (ddd, 1H, J = 1.1 Hz, J = 7.3 Hz, J = 7.5 Hz, H-4), 4.70 (s, 1H, H-7); ^{13}C NMR ($CDCl_3$, 125 MHz) δ 153.0 (s, C-1), 144.1 (s, C-8), 139.6 (s, C-15), 138.0 (s, C-13), 130.0 (d), 129.0 (d), 128.64 (d), 128.57 (d), 128.03 (d), 128.00 (s), 127.9 (d), 127.6 (d), 127.11 (s, C-6), 127.06 (d, C-5), 127.0 (d, C-10), 124.3 (d, C-9), 120.8 (d, C-4), 120.2 (d, C-2), 82.5 (s, C-14), 52.7 (d, C-7); MS (EI) *m*/*z* 347 (M^+, 30), 346 (M^+, 100), 252 (15); HRMS calculated for $C_{26}H_{18}O$ 346.1358, observed 346.1360.

Laser Flash Photolysis (LFP). All LFP studies were conducted at the University of Victoria LFP facility employing a YAG laser, with a pulse width of 10 ns and excitation wavelength 355 nm. Flow cells (0.7 cm) were used and solutions were purged with nitrogen or oxygen for 30 min prior to measurements. Optical densities at 355 nm were ~0.4.

Steady-State and Time-Resolved Fluorescence Measurements. The samples were dissolved in CH_3CN and the concentrations were adjusted to have optical densities at the excitation wavelength (355 or 375 nm) <0.1. Solutions were purged with nitrogen for 15 min prior to analysis. The measurements were performed at 20 °C and were not corrected. Fluorescence quantum yields were determined by comparison of the integral of emission bands with that of quinine bisulfate (Φ = 0.55 in 1.0 N H_2SO_4).[10] Typically three absorption traces were recorded (and averaged) and two fluorescence emission traces, exciting at two different wavelengths (i.e., 355 and 375 nm). Two quantum yields were calculated and the mean value reported.

Fluorescence decay histograms were obtained on an instrument equipped with a hydrogen flash lamp, using the time-correlated single photon counting technique in 1023 channels. Histograms of

the instrument response functions (using a LUDOX scatterer) and sample decays were recorded until they typically reached 3×10^3 counts in the peak channel. The half width of the instrument response function was typically ~1.5 ns. The time increment per channel was 0.049 or 0.098 ns. Obtained histograms were fitted as sums of the exponential, using Gaussian-weighted nonlinear least-squares fitting based on Marquardt−Levenberg minimization implemented in the software package of the instrument. The fitting parameters (decay times and preexponential factors) were determined by minimizing the reduced χ_g^2. An additional graphical method was used to judge the quality of the fit that included plots of surfaces ("carpets") of the weighted residuals vs channel number.

Acknowledgment. Support of this work was provided by the National Sciences and Engineering Research Council (NSERC) of Canada.

Supporting Information Available: Detailed experimental procedures, ^{1}H and ^{13}C NMR spectra of the isolated compounds, ^{1}H NMR spectra of some representative photochemical reaction mixtures, UV and fluorescence spectra of **7**−**10**, and representative LFP runs. This material is available free of charge via the Internet at http://pubs.acs.org.

JO0524728